A&A 460, L49–L52 (2006)
DOI: 10.1051/0004-6361:20066559

Astronomy & Astrophysics

Letter to the Editor

High resolution observations of a starburst at $z = 0.223$: resolved CO(1–0) structure⋆

F. Combes[1], S. García-Burillo[2], J. Braine[3], E. Schinnerer[4], F. Walter[4], L. Colina[5], and M. Gerin[6]

[1] Observatoire de Paris, LERMA (CNRS: UMR8112), 61 Av. de l'Observatoire, 75014, Paris, France
e-mail: francoise.combes@obspm.fr
[2] Observatorio Astronómico Nacional (OAN), Observatorio de Madrid, Alfonso XII, 3, 28014 Madrid, Spain
[3] Observatoire de Bordeaux, Université Bordeaux I, BP 89, 33270 Floirac, France
[4] Max-Planck-Institut für Astronomie (MPIA), Königstuhl 17, 69117 Heidelberg, Germany
[5] IEM, Consejo Superior de Investigaciones Cientificas (CSIC), Serrano 121, 28006 Madrid, Spain
[6] Radioastronomie ENS, 24 rue Lhomond, 75005 Paris, France

Received 13 October 2006 / Accepted 27 October 2006

ABSTRACT

We present the results of mapping the CO(1–0) emission of the $z = 0.223$ ultra-luminous starburst IRAS 11582+3020, with the IRAM interferometer, at ∼1″ resolution. This galaxy was selected from an IRAM-30 m survey of 30 galaxies at moderate redshift ($z \sim 0.2$–0.6) to explore galaxy evolution and, in particular, the efficiency of star formation, in the redshift range filling the gap between local and very high-z objects. The CO emission is kinematically resolved, and about 50% of the total emission found in the 27″ (97 kpc) single dish beam is not recovered by the interferometer. This indicates that some extended emission may be present on large scales (typically 7–15″). The FIR-to-CO luminosity ratio follows the trend from local to high-z ultra-luminous starbursts.

Key words. galaxies: general – galaxies: high redshift – galaxies: ISM – galaxies: starburst – radio lines: galaxies

1. Introduction

The star formation history (SFH) of the Universe has been extensively studied in recent years through high spatial resolution observations of star-forming galaxies as a function of look-back time (e.g. Madau et al. 1998). The main striking feature is a steady increase in the star formation rate between $z = 0$ and $z = 1$, by at least a factor 10 and usually even more (Blain et al. 1999a).

Starbursts were more frequent in the recent past, and star-forming regions were also more dust enshrouded – the evolution of galaxies appears to be much faster in the infrared than in the optical/UV. This strong evolution of infrared-bright star-forming galaxies is not really understood in models of galaxy evolution. It has been established observationally that the number of galaxy mergers that trigger starbursts increases with redshift as a high power law, like $(1 + z)^3$ (e.g. Le Fèvre et al. 2000), which is consistent with numerical simulations and semi-analytical models (e.g. Balland et al. 2003). However, to reproduce the strong SF evolution, the contribution of mergers to the star-formation and their efficiency must also vary considerably with redshift, with a peak at $z \sim 1$, to agree with the observations (cf. Blain et al. 1999b; Combes 1999).

To better understand the physics responsible for this evolution, it is paramount to measure the content and distribution of the fuel for star formation, i.e. the molecular gas, as a function of redshift. Although a few tens of ultra-luminous infrared galaxies, often amplified by a gravitational lens, have been mapped in the CO line at very high redshift (e.g. Omont et al. 2003; Walter et al. 2004; Tacconi et al. 2006), not much is known about star-forming galaxies at moderate distances, in the range $0.2 < z < 0.6$ (only 2 objects have been studied in this range, Solomon et al. 1997). Therefore, we have undertaken a CO survey of 30 IR-luminous galaxies in this redshift range to check whether the derived molecular gas content and star formation efficiency (SFE or SFR/M(H_2)) are evolving at this faster rate as well.

For this study, we first obtained global information on the molecular content and on the SFE using single-dish data[1]. After a successful detection in our single-dish survey, we obtained high-resolution Plateau de Bure Interferometer (PdBI) observations to map the molecular gas distribution. Resolving the gas distribution and kinematics is crucial for attributing the star formation activity either to a global merger or a less violent process. The first high-resolution CO observations of the survey were obtained towards IRAS 11582+3020, which is the object of this Letter.

2. The sample and the source IRAS 11582+3020

The ULIRG sample of Solomon et al. (1997) contains 37 objects, but only 2 have $z > 0.2$. To fill the gap between low and high-z ($z > 2$) studies, we initiated the first systematic survey of $0.2 < z < 0.6$ sources, selecting the 30 most luminous galaxies detected at 60 micron (IRAS or ISO) with known spectroscopic redshifts. IRAS 11582+3020 is one of the 12 best-detected galaxies. It is an ultra-luminous galaxy with $L(\mathrm{IR}) = 5.4 \times 10^{12}\ L_\odot$ (with an IR flux computed from

⋆ Based on observations carried out with the IRAM Plateau de Bure Interferometer. IRAM is supported by INSU/CNRS (France), MPG (Germany), and IGN (Spain).

[1] An article presenting the results of our galaxy survey will be presented elsewhere, Combes et al. in prep.

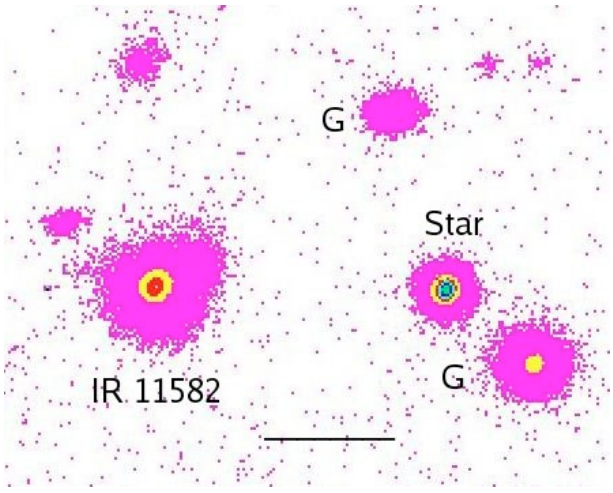

Fig. 1. Red image of IRAS 11582+3020 from Kim et al. (2002). The two objects marked "G" are galaxies in the same group (a foreground star is also indicated). The length of the horizontal bar at the bottom is $10'' = 36$ kpc at $z = 0.223$.

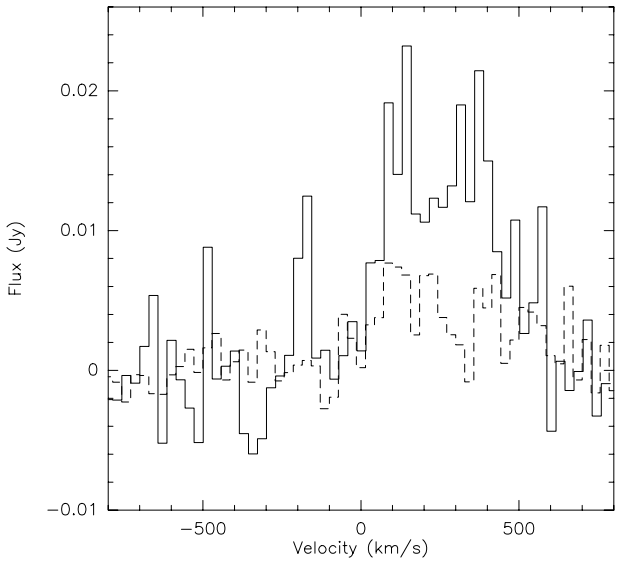

Fig. 2. The IRAM 30 m CO(1–0) spectrum (solid line), compared with the integrated spectrum from the interferometer (dashed line). The velocity is relative to $z = 0.223$.

IR $= 1.8 \times (13.48\, f_{12} + 5.16\, f_{25} + 2.58\, f_{60} + f_{100})\ 10^{-14}$ W m^{-2}; Sanders & Mirabel 1996). Based on the ion lines in its optical spectrum, it was classified as a LINER by Kim et al. (1998). The source is not detected in the 2 cm radio continuum by the VLA, with an upper limit of 0.8 mJy (Nagar et al. 2003), but it is a 20 cm radio-source with a flux of 3 mJy (Becker et al. 1995). The FIR-to-radio ratio $q = \log([F_{\rm FIR}/(3.75 \times 10^{12}\ {\rm Hz})]/[f_\nu(1.4\ {\rm GHz})]) = 2.7$, as is typical of ULIRGs (Sanders & Mirabel 1996). Rupke et al. (2005) find evidence of a superwind outflow in this galaxy of about 15 $M_\odot$ yr^{-1}, while its SFR is estimated at 740 $M_\odot$ yr^{-1} from the infrared luminosity, $SFR = \alpha\ L_{\rm IR}/(5.8 \times 10^9\ L_\odot)$ (e.g. Kennicutt 1998), using a correction factor of $\alpha = 0.8$ for the AGN contribution, as adopted by Rupke et al. (2005). The red image of Kim et al. (2002) reveals some extended diffuse emission, while two galaxies of the same group (according to the spectroscopy by Veilleux et al. 2002) are within 90 kpc in projection (Fig. 1). Veilleux et al. (2002) classify this system as a post-merger; i.e. the tidal tails have been so diluted that they become barely visible, while the center is still perturbed, with a prominent knot of star formation.

In this article, we adopt a standard flat cosmological model, with $\Lambda = 0.7$, and a Hubble constant of 70 km s^{-1} Mpc^{-1}. IRAS 11582+3020 at $z = 0.223$ then has an angular distance of 743 Mpc and $1'' = 3.6$ kpc. The luminosity distance is 1111 Mpc.

3. Observations

First, we performed IRAM 30m observations in May 2005 (see Fig. 2). We used 2 SIS receivers to observe the 2 polarizations simultaneously at 94.253 GHz, which is the redshifted frequency of the CO(1–0) line. At this frequency, the telescope's half-power beam width is $27''$. The main-beam efficiency is $\eta_{\rm mb} = T_{\rm A}^*/T_{\rm mb} = 0.77$ and $S/T_{\rm A}^* = 6.1$ Jy/K. The typical system temperature was 120 K (on the $T_{\rm A}^*$ scale). Wobbler switching mode was used, with reference positions offset by $2'$ in azimuth. Two 1 MHz filter banks provided a total bandwidth of 512 MHz, or 1600 km s^{-1}, with a velocity resolution of 3.2 km s^{-1}.

IRAS 11582+3020 was subsequently observed with the 6 antennae of the PdBI in January and February 2006 in the new A and B configurations. The 3 mm receiver was tuned to 94.253 GHz and the 1 mm to 240 GHz for the dust continuum (as no other CO line falls in the tuning bands). The dual-band SIS receivers yielded SSB receiver temperatures around 40 K and 50 K at the two observed frequencies. The system temperatures were 120 K for CO(1–0) and 400 K at 240 GHz. Four correlator units covered a total bandwidth of 580 MHz at each frequency, providing a nominal frequency resolution of 1.25 MHz (4 km s^{-1} for the CO(1–0) line); however, we smoothed the signal to 28.6 km s^{-1} channels. On average, the residual atmospheric phase jitter was less than 20° at 3 mm, consistent with a seeing disk of $0.34''$–$0.46''$ size and with a ∼5% loss of efficiency.

Reduction using the GILDAS software provided data cubes with 512×512 spatial pixels ($0.14''$/pixel) and 64 velocity channels of 28.6 km s^{-1} width. The cubes were cleaned with the Clark (1980) method and restored by a $1.3'' \times 1.0''$ Gaussian beam (with PA = 54°) at 94.253 GHz and $0.43'' \times 0.25''$ (with PA = 44°) at 240 GHz. The rms noise levels in the cleaned maps (at 28.6 km s^{-1} velocity resolution) are 0.8 mJy beam^{-1} for the CO(1–0) line. No continuum emission was detected at 3 mm (possible AGN) or at 1 mm (possible dust emission), down to rms noise levels of 0.1 mJy beam^{-1} and 0.5 mJy beam^{-1} in a 580 MHz bandwidth at 94 GHz and 240 GHz, respectively. Given the IRAS 100 μm flux of 1.5 Jy, the upper limit at 1.2 mm is compatible with a typical starburst SED.

4. Results

As revealed in Fig. 2, the total PdBI flux is ∼50% of what is found with the single dish. When taking the intrinsic flux uncertainties into account, this may indicate that some extended emission is not recovered by our interferometer observations. With a beam of $27''$ at the 30 m, we measured a CO(1–0) flux toward the center of $I({\rm CO}) = 1.3$ K km s^{-1} (in the $T_{\rm A}^*$ scale). With a conversion factor of 6.1 Jy/K, the integrated flux is then $S({\rm CO}) = 7.8$ Jy km s^{-1}. With the PdBI, we measured 3.7 Jy km s^{-1} in the FOV = $54''$ of the CO(1–0) map. This can be explained by the long PdBI baselines that are not sensitive to CO emission extending over $10''$ and that detect only the more clumpy distribution. The optical structure does reveal the existence of such an extended component, and also hints at a weak

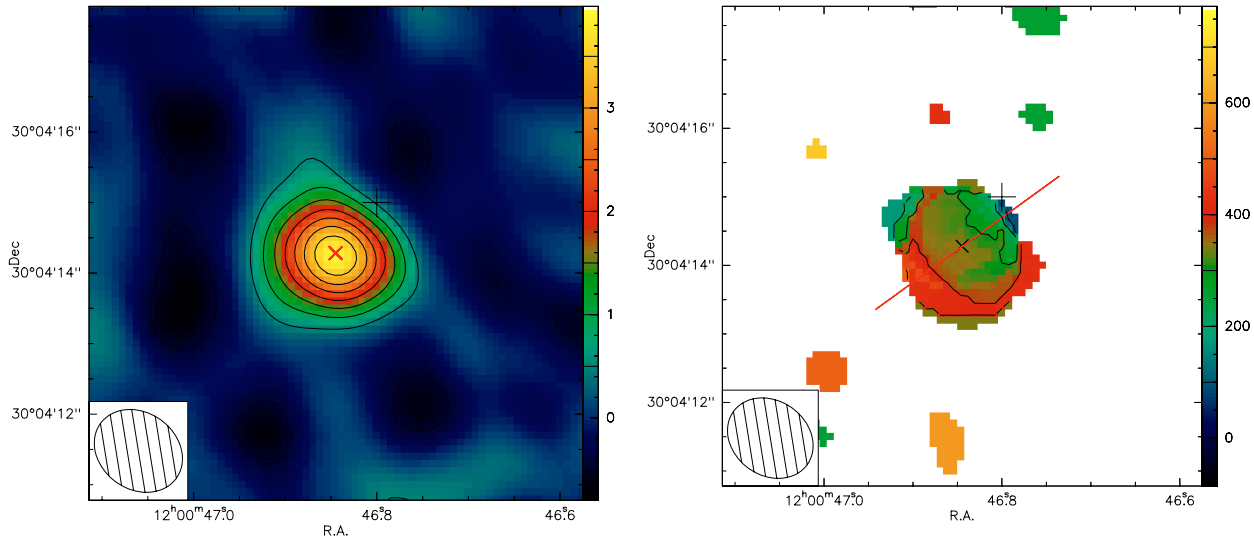

Fig. 3. a) CO(1–0) integrated intensity contours in the inner ~7″ (25.2 kpc) of IRAS 11582+3020. Contours are −0.5, 0.5 to 4 Jy km s^{-1} beam^{-1} in steps of 0.5 Jy km s^{-1} beam^{-1} (1-σ = 0.2 Jy km s^{-1} beam^{-1}). The black cross marks the position of the phase tracking center (α_{J2000} = 12^{h}00^{m}46.8^s and δ_{J2000} = 30°04′15.0″). The red cross marks the position of the CO peak intensity and CO-based dynamical center (α_{J2000} = 12^{h}00^{m}46.85^s and δ_{J2000} = 30°04′14.3″). **b)** The mean velocity field derived from the 1–0 data using a 3σ-clipping in each channel map, in line contours, spanning the range (100 km s^{-1}, 500 km s^{-1}) in steps of 100 km s^{-1}. The velocity scale is relative to z = 0.223 with a CO-derived systemic velocity of v_{sys} = 300 km s^{-1}, i.e., z_{CO} = 0.224 (redhifted by 180 km s^{-1} from the optical line that is at z = 0.2234). The red line shows the position of the apparent major axis of the galaxy. Beam-sizes are represented by hatched ellipses.

Table 1. CO results from IRAM-30 m and PdBI, and deduced H_2 mass (ΔV is the *FWHM*).

Instrument	ΔV km s^{-1}	Area Jy km s^{-1}	$M(H_2)$ $M_\odot$
30 m	476 ± 33	7.8 ± 0.5	1.2 ± 0.1 × 10^{10}
PdBI	550 ± 52	3.7 ± 0.3	6 ± 0.4 × 10^9

diffuse tidal tail in this perturbed system, classified as a post-merger (Veilleux et al. 2002).

The CO luminosity for a high-z source is given by

$$L_{CO} = 23.5 I_{CO} \Omega_B \frac{D_L^2}{(1+z)^3} \quad \text{K km s}^{-1} \text{ pc}^2$$

where Ω_B is the area of the main beam in square arcseconds and D_L = 1111 is the luminosity distance in Mpc. We computed H_2 masses by $M_{H_2} = \alpha L_{CO}\ M_\odot$, with α = 0.9 for ULIRGs, instead of 4.6 for normal galaxies (i.e. Solomon et al. 1997). The molecular masses are listed in Table 1.

The integrated CO(1–0) map is plotted in Fig. 3, together with the isovelocity curves. The source is resolved at least in the direction of the beam's minor axis, where the deconvolved size of the CO emitting region is of the order of 0.8″ in diameter (~3 kpc). The signal-to-noise ratio is around 10 in most of the channels, implying a precision of ~0.1″ on the position of the peaks. Therefore it is possible to detect the shift of the barycenter in each channel map, with a kinematic major axis aligned at PA ~ 135° (Fig. 3). The velocity gradient is also clearly seen in the position-velocity diagram taken along this position angle (Fig. 4). Since ~135° is also the position angle of the extended optical isophotes (Fig. 1), all available data are compatible with a post-merger relaxed system.

The CO integrated spectrum seems to show a double-horn profile, indicative of a rotating disk. Since the contours of the red image suggest an inclination of i = 50° with the plane of the sky

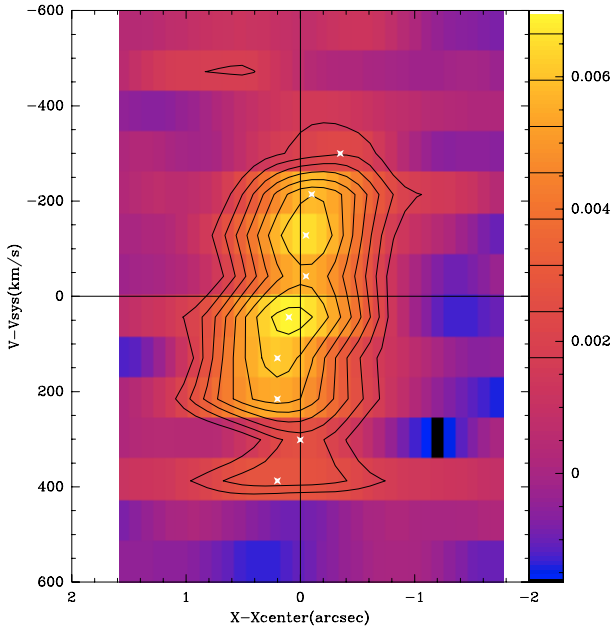

Fig. 4. We show the CO(1–0) position-velocity diagram along the major axis of IRAS 11582+3020 (line contour range: 2.5σ, to 10.5σ in steps of 1σ; 1σ = 0.7 mJy beam^{-1} in channels of 86 km s^{-1}). Velocities have been re-scaled to z_{CO} = 0.224, and angular offsets are relative to the dynamical center. The white crosses mark the velocities corresponding to the peak brightness temperatures as a function of position.

for a disk geometry, we can estimate a dynamical mass, by assuming that the width of the CO profile is twice the projected rotational velocity $V_{rot} \sin i$ = 250 km s^{-1}. With V_{rot} = 326 km s^{-1} inside a radius of 1.5 kpc, i.e. the extent of the central molecular disk, the indicative dynamical mass is $M_{dyn} = 3.4 \times 10^{10}\ M_\odot$. With the low conversion ratio proposed for the ULIRGs, the gas mass in the central molecular disk ($M(H_2) = 6 \times 10^9\ M_\odot$) is a small fraction (~20%) of the dynamical mass inside 1.5 kpc.

5. Discussion and conclusions

The ∼1″ resolution CO observations of the ultra-luminous starburst IRAS 11582+3020 at $z = 0.223$ provides interesting insight into its molecular gas content and morphology. The CO emission is resolved, both spatially and kinematically: we see evidence of a rotating disk. In addition to a central molecular disk of ∼1.5 kpc in radius, there is tentative evidence of additional extended emission over 10–15″ since about 50% of the 30m flux is not recovered by the interferometer. Such an extended component could correspond to the perturbed optical morphology of the evolved merger. This source size contrasts with the 10 nearby ULIRGs, mapped by Downes & Solomon (1998), where the molecular gas is more concentrated, with typical radii of 300 to 800 pc. The total amount of molecular gas derived in IRAS 11582+3020 is comparable to the average mass in local ULIRGs of $\sim 5 \times 10^9\ M_\odot$, and its $M_{\rm gas}/M_{\rm dyn}$ ratio is also comparable to the value of ∼1/6 found by Downes & Solomon (1998).

The physical properties of IRAS 11582+3020 appear to be intermediate between those of local ULIRGs and high-z submillimeter galaxies (SMG) as mapped by Tacconi et al. (2006). The latter also have a typical radius of 2 kpc, and their FIR-to-CO luminosity ratio is higher than the local ULIRGs ratio, due to their higher FIR luminosities. There might be a trend, also followed by IRAS 11582+3020, for high-z galaxies to have a higher $L(\mathrm{FIR})/M(\mathrm{H_2})$ ratio (Riechers et al. 2006), however this must be confirmed with larger samples. The high-z SMG of Tacconi et al. (2006) are only mapped in the higher J rotation lines of CO, which may explain the complete absence of extended emission, even in the case of mergers. From their study of the three CO-brightest $z \geq 4$ QSOs, Riechers et al. (2006) limit a potentially extended CO emission to <30% of the total. Two of their quasars are gravitationally lensed (with magnification factors of ∼3–7), i.e. differential magnification may slightly increase this limit.

Acknowledgements. The authors gratefully acknowledge P. Salomé for his help in the interferometric data reduction and D.-C. Kim for having provided the red and K' images of IRAS 11582+3020. We made use of the NASA/IPAC Extragalactic Database (NED).

References

Balland, C., Devriendt, J., & Silk, J. 2003, MNRAS, 343, 107
Becker, R. H., White, R. L., & Helfand, D. J. 1995, ApJ, 450, 559
Blain, A. W., Smail, I., Ivison, R. J., & Kneib, J.-P. 1999a, MNRAS, 302, 632
Blain, A. W., Jameson, A., Smail, I., et al. 1999b, MNRAS, 309, 715
Combes, F. 1999, Ap&SS, 269, 405
Downes, D., & Solomon, P. 1998, ApJ, 507, 615
Kennicutt, R. C. 1998, ApJ, 498, 541
Kim, D. C., Veilleux, S., & Sanders, D. B. 1998, ApJ, 508, 627
Kim, D. C., Veilleux, S., & Sanders, D. B. 2002, ApJS, 143, 277
Le Fèvre, O., Abraham, R., Lilly, S. J., et al. 2002, MNRAS, 311, 565
Madau, P., Pozzetti, L., & Dickinson, M. E. 1998, ApJ, 498, 106
Nagar, N. M., Wilson, A. S., Falcke, H., et al. 2003, A&A, 409, 115
Omont, A., Cox, P., Beelen, A., Bertoldi, F., & Carilli, C. L. 2003, AGN from Central Engine to Host Galaxy, PASP, 290, 583
Riechers, D. A., Walter, F., Carilli, C., et al. 2006, AJ, 650, 604
Rupke, D. S., Veilleux, S., & Sanders, D. B. 2005, ApJS, 160, 115
Sanders, D. S., & Mirabel, F. 1996, ARA&A, 34, 749
Solomon, P., Downes, D., Radford, S., & Barrett, J. 1997, ApJ, 478, 144
Tacconi, L. J., Neri, R., Chapman, S. C., et al. 2006, ApJ, 640, 228
Veilleux, S., Kim, D.-C., & Sanders, D. B. 2002, ApJS, 143, 315
Walter, F., Carilli, C., Bertoldi, F., et al. 2004, ApJ, 615, L17